



Supplement of

Recommendations for using core X-ray fluorescence data on basaltic rock as a tool to assess compositional variability

Ashley M. Morris et al.

Correspondence to: Ashley M. Morris (ashley.m.morris@utah.edu)

The copyright of individual parts of the supplement might differ from the article licence.

Contents of this file

Section S1 Small-scale variability for Holes U1571A and U1574A

Captions for Tables S1 to S3

Figures S1 to S5

Introduction

Text provided here includes information that is supplemental to that provided in the main text as well as additional, supplementary figures. Additional supplemental tables are uploaded into a single, separate Excel file, and full core section photos referenced by Figure 6 are uploaded in a separate zip file with file names formatted as “U1566A-6R2” for Site U1566, Hole A, Core 6, Section 2 on Zenodo (DOI: [10.5281/zenodo.18343315](https://doi.org/10.5281/zenodo.18343315)).

S1 Small-scale variability for Holes U1571A and U1574A

The calibrated XRF-cs chemical stratigraphy for Hole U1571A highlights chemical anomalies within sections of continuous aphyric basalt (negative Ti and Sr at 215.19–216.16 m, CSF-A; Fig. S4) and plagioclase phyric basalt (positive Zr at 240.97–242.33 m, CSF-A; Fig. S3). For the section of aphyric basalt, the uncalibrated intensity ratios of the uncalibrated dataset are more difficult to distinguish from the surrounding data. The uncalibrated XRF-cs data does show a negative Ti/Zr anomaly in the plagioclase phyric basalt section, as well as Ni/Mn trend that decreases downhole (Fig. S3). The calibrated XRF-cs chemical stratigraphy for Hole U1574A shows more broad trends in relatively continuous sections of aphyric and plagioclase phyric basalt, where Ti, Sr, and Zr gradually increase and Ni gradually decreases downhole (169.83–205.74 m, CSF-A; Fig. S4). Similar trends can be observed by the uncalibrated XRF-cs data, where Ti/Zr increases and Sr/Zr decreases downhole, however, Ni/Mn values are relatively consistent for the same section (Fig. S3).

Supplementary Table Captions

Table S1: XRF-core scanning data for Holes U1566A, U1571A, and U1574A.

Table S2: pXRF data used for calibration from Holes U1566A, U1571A, and U1574A.

Table S3: ANOVA and Tukey HSD test results.

Supplementary Figures

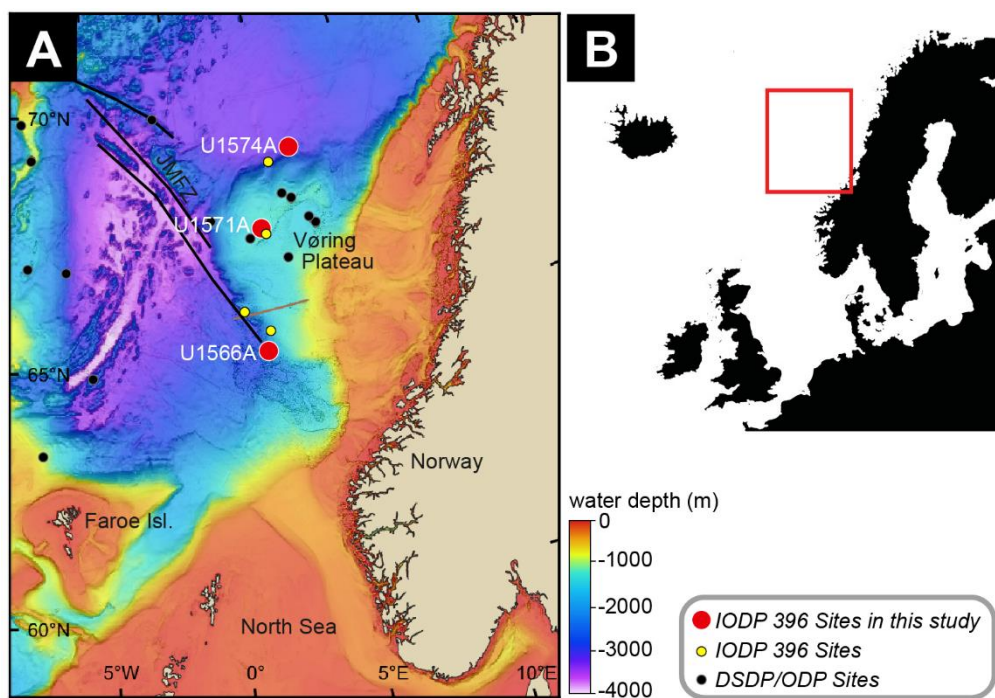


Figure S1: (A) Map of IODP Expedition 396 Sites and nearby DSDP and ODP Sites (Planke et al., 2023b). (B) Map of the eastern side of the North Atlantic, the red box outlines the area represented in A.

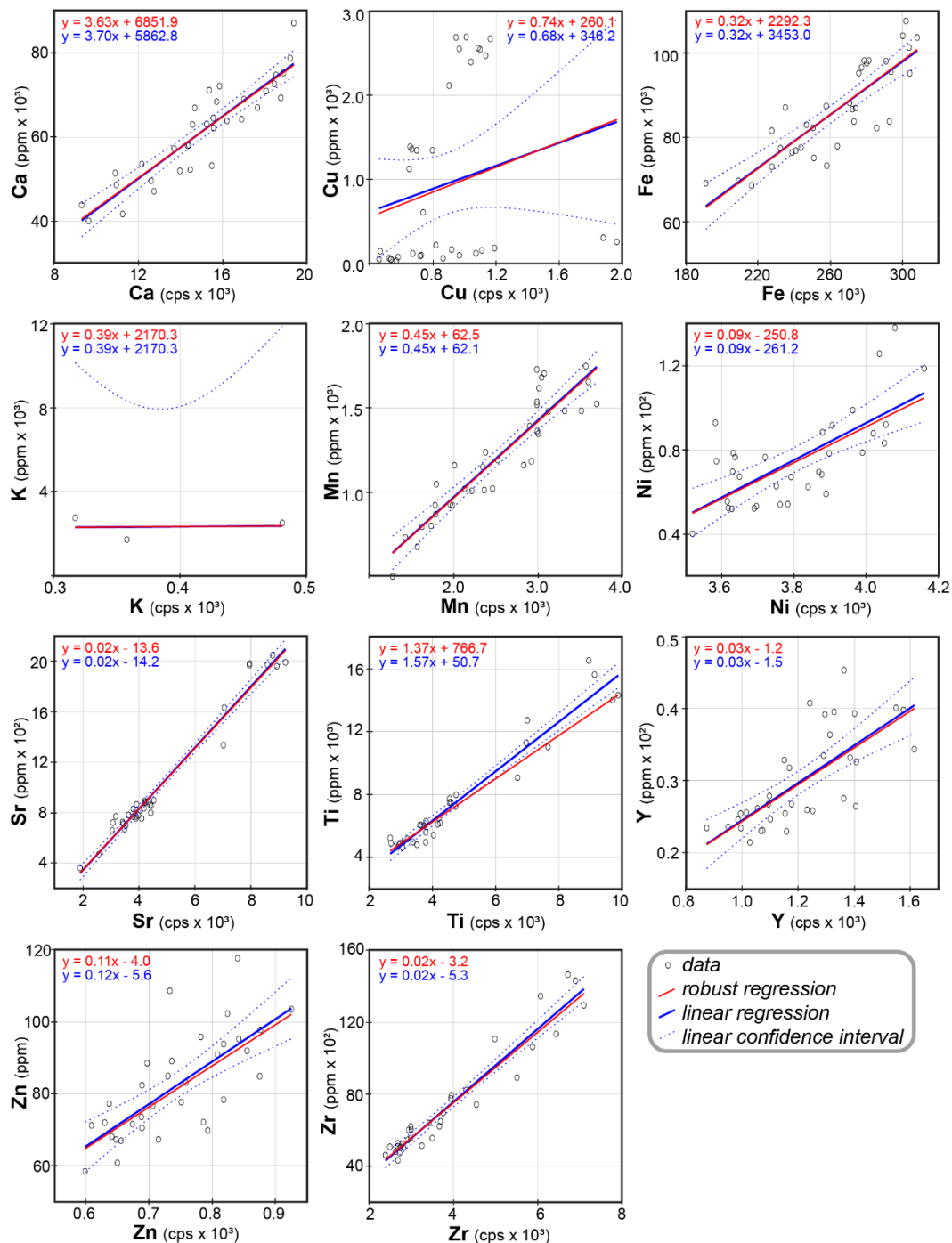


Figure S2: Calibration curves for calibrating the XRF-cs raw intensity (cps) data using discrete pXRF analyses (Tegner et al. 2025). Both linear and robust regression curves are shown; only the robust regression curves are used as described in Section 3.2.

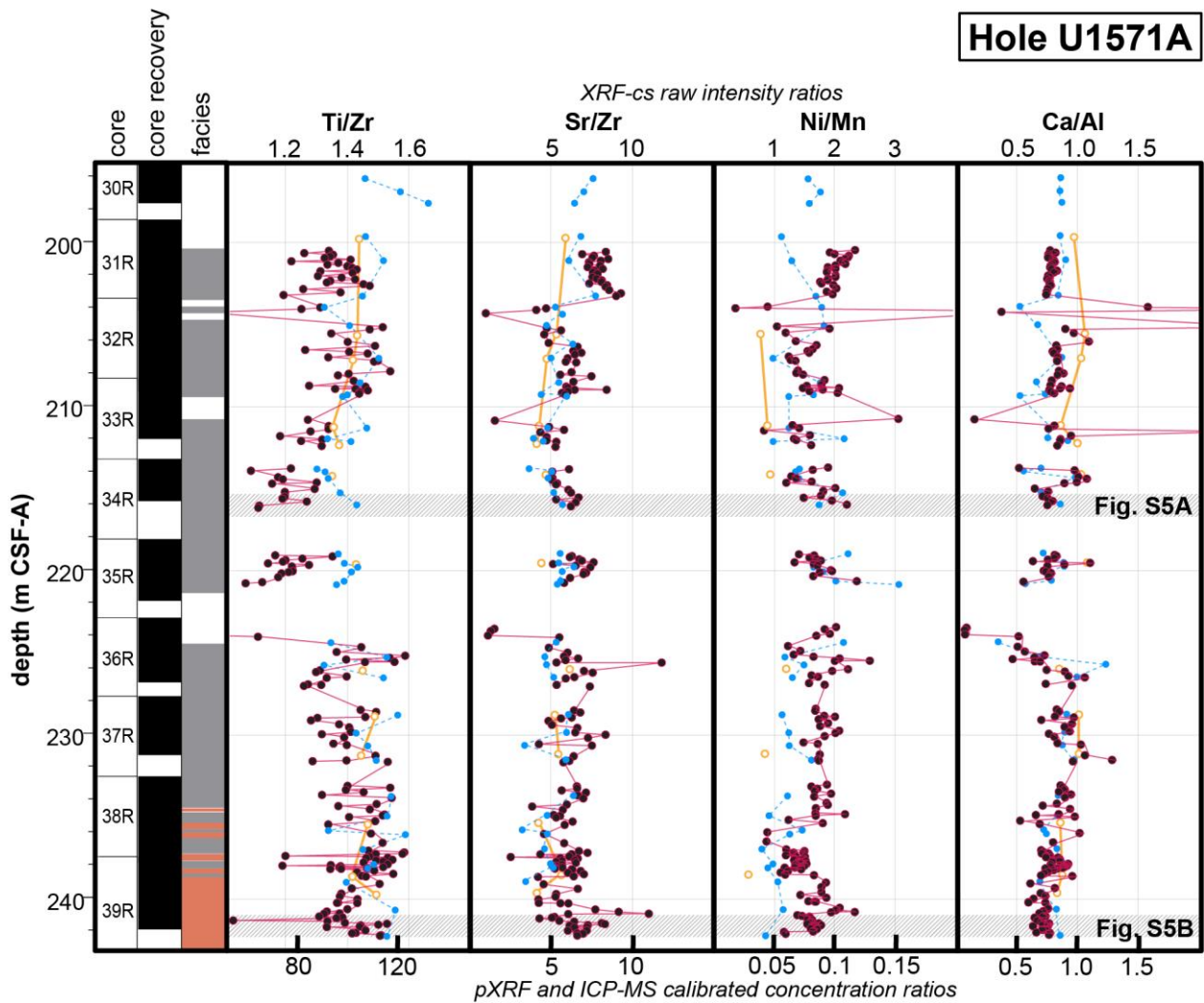


Figure S3: Chemical stratigraphy for Ti/Zr, Sr/Zr, Ni/Mn, and Ca/Al element intensity (cps) ratios for basalts from Holes U1571A and U1574A measured by the XRF-cs. The pXRF and ICP-MS concentration (ppm) ratios (Tables S2, S3; Tegner et al. 2025) are also plotted. For the XRF-cs and pXRF data, “cal” denotes analyses that were used to calculate the calibration curves (Fig. S2). Gray hatched sections indicate sections of core discussed in the text with corresponding core photos in Figure S5. Lithologies are from the shipboard IODP Expedition 396 observations (Planke et al., 2023b).

Hole U1574A

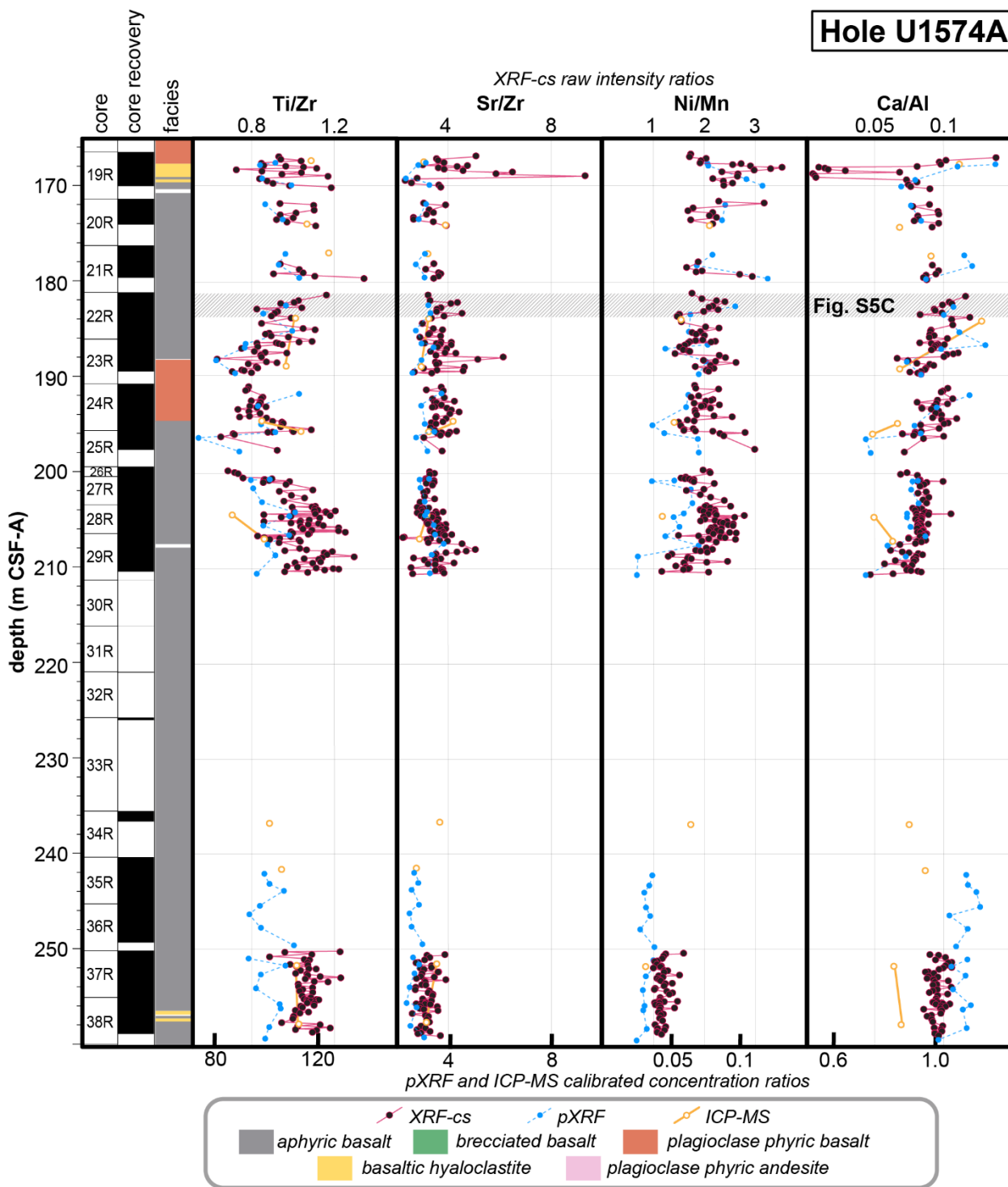


Figure S3: Continued.

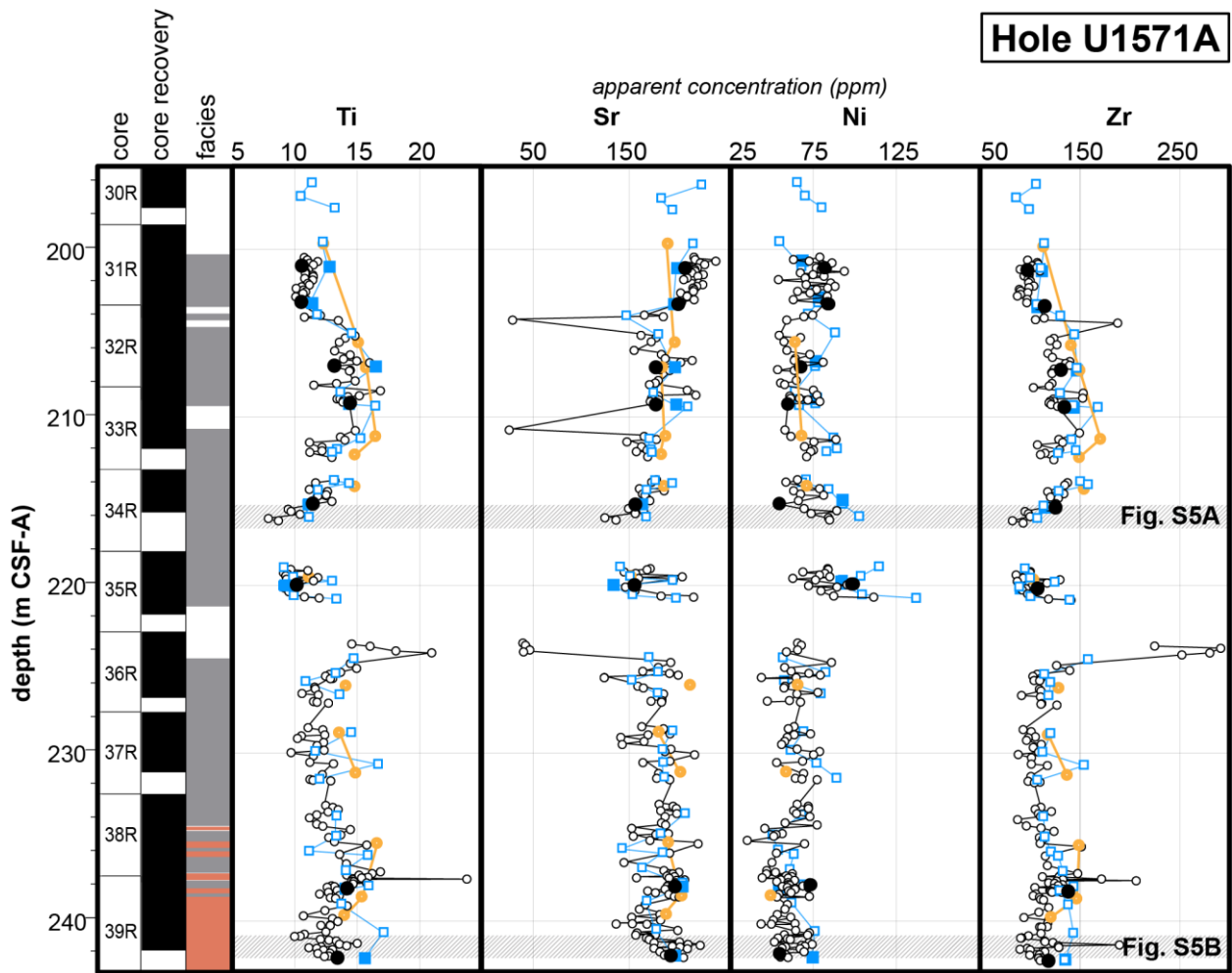


Figure S4: XRF-cs measured Ti, Sr, Ni, and Zr calibrated concentration (ppm) chemical stratigraphy plots for basalts from Holes U1571A and U1574A. The pXRF and ICP-MS concentration (ppm) data (Tables S2, S3; Tegner et al. 2025) are also plotted for each site. Gray hatched sections indicate sections of core discussed in the text with corresponding core photos in Figure S5. Lithologies are from the shipboard IODP Expedition 396 observations (Planke et al., 2023b).

Hole U1574A

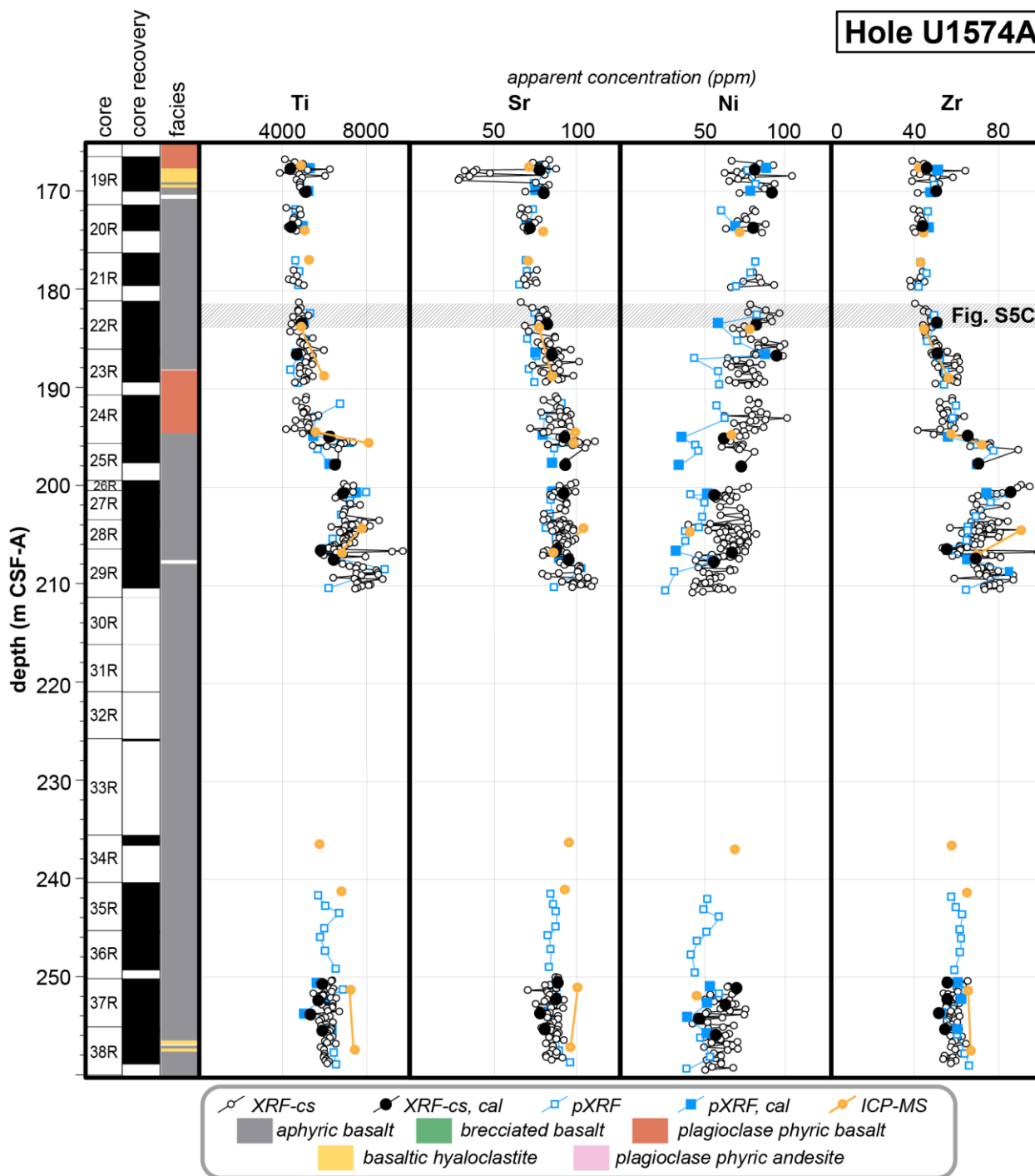


Figure S4: Continued.

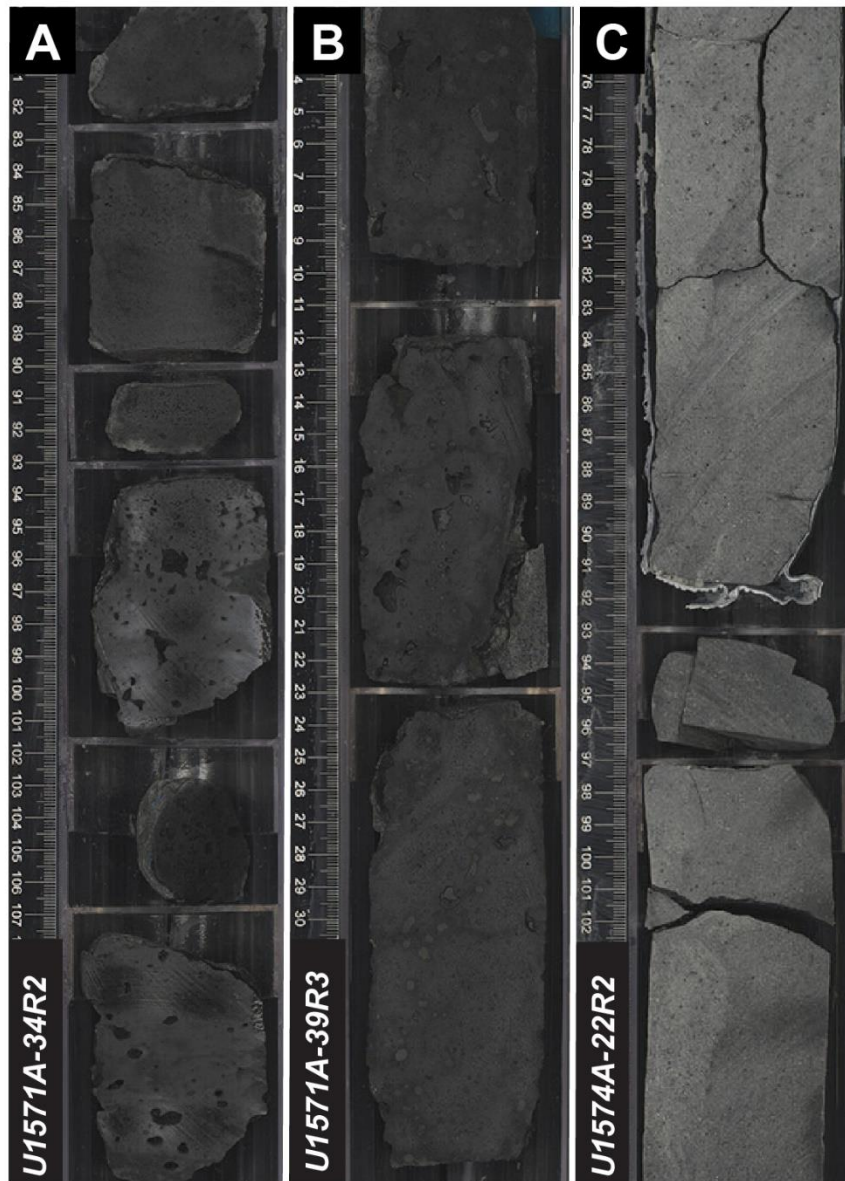


Figure S5: Photos of representative pieces of sections of the cores described within the text. (A) U1571A-34R2 (215.19–216.16 m, CSF-A) is a section of continuous aphyric basalt and (B) U1571A-39R3 (240.97–242.33 m, CSF-A) is a section of plagioclase phyric basalt. (C) U1574A-22R2 (182.79–183.74 m, CSF-A) is a representative section of aphyric basalt that appears homogenous and is chemically homogenous (Figs. S3, S4).